The Microrheology of Sickle Hemoglobin Gels

ARTICLE *in* BIOPHYSICAL JOURNAL · AUGUST 2010

Impact Factor: 3.97 · DOI: 10.1016/j.bpj.2010.04.079 · Source: PubMed

4 AUTHORS, INCLUDING:

Mikhail N Zakharov
National Institutes of Health
17 PUBLICATIONS **144** CITATIONS
SEE PROFILE

Alexey Aprelev
Drexel University
33 PUBLICATIONS **204** CITATIONS
SEE PROFILE

Frank A Ferrone
Drexel University
96 PUBLICATIONS **2,387** CITATIONS
SEE PROFILE

The Microrheology of Sickle Hemoglobin Gels

Mikhail N. Zakharov,[†] Alexey Aprelev,[†] Matthew S. Turner,[‡] and Frank A. Ferrone[†*]
[†]Department of Physics, Drexel University, Philadelphia, Pennsylvania; and [‡]Department of Physics, University of Warwick, Coventry, United Kingdom

ABSTRACT Sickle cell disease is a rheological disease, yet no quantitative rheological data exist on microscopic samples at physiological concentrations. We have developed a novel method for measuring the microrheology of sickle hemoglobin gels, based on magnetically driven compression of 5- to 8-μm-thick emulsions containing hemoglobin droplets ~80 μm in diameter. Using our method, by observing the expansion of the droplet area as the emulsion is compressed, we were able to resolve changes in thickness of a few nanometers with temporal resolution of milliseconds. Gels were formed at various initial concentrations and temperatures and with different internal domain structure. All behaved as Hookean springs with Young's modulus from 300 to 1500 kPa for gels with polymerized hemoglobin concentration from 6 g/dl to 12 g/dl. For uniform, multidomain gels, Young's modulus mainly depended on the terminal concentration of the gel rather than the conditions of formation. A simple model reproduced the quadratic dependence of the Young's modulus on the concentration of polymerized hemoglobin. Partially desaturated samples also displayed quadratic concentration dependence but with a smaller proportionality coefficient, as did samples that were desaturated in steps; such samples were significantly less rigid than gels formed all at once. The magnitude of the Young's modulus provides quantitative support for the dominant models of sickle pathophysiology.

INTRODUCTION

Sickle cell disease occurs because a genetic mutation of hemoglobin permits it to polymerize under deoxygenated conditions. These polymers rigidify the normally pliable red cell, blocking blood flow and delivery of oxygen and thus causing pain and organ damage. It is thus evident that the disease is fundamentally controlled by the rheological properties of the hemoglobin polymers that form in the cell.

The bulk rheology of polymerized hemoglobin solutions, also described as gels, has been explored by a number of investigators (1–3), with early work focused as much on deciphering the mechanism of gel formation as on quantitative measurement of gel properties. An important distinction was made quite early by Briehl, who observed that since polymer gels hold a stress indefinitely, they are better described as solid than gel (1). In his experiments, the shear modulus was found to be <1 kPa, a value that is dramatically less than the stiffness of individual fibers, now known to be some 10^5 times greater (4,5). These measurements were associated with gels formed from relatively low initial concentrations (e.g., ~22 g/dl), and the resulting small polymer mass (~3 g/dl) might account for the weakness of the gels. Physiological gels, in contrast, can be more substantial (e.g., ~11 g/dl). The small mass is an inherent limit of bulk measurements using temperature jump to induce gelation. To illustrate, the solubility of a gel is 28.5 g/dl at 4°C, so that at best, one could prepare a sample that yields 8 g/dl of polymer, still below physiological conditions, even assuming that the containing rheometer could have its temperature raised from 4° to ~25°C in less than the 1–2 s it would take to form polymers in a sample of that concentration. Moreover, thermal gradients during polymerization could affect the gel microstructure, which arises from the polymerization mechanism itself. Polymers form in a process of double nucleation (6). Deoxyhemoglobin (deoxyHb) monomers in a solution devoid of polymers at a concentration above solubility are more stable than small aggregates, but not more stable than large polymers. Polymer formation must proceed by initial formation of small, unstable aggregates, the least stable of which is the nucleus. If polymers already exist in the solution, their surface can help stabilize the unstable aggregates, which allows new polymers to nucleate on the surface of others in a process called heterogeneous nucleation. The heterogeneous process causes polymers to grow naturally and inevitably in attached arrays, called domains. Every domain begins from a single homogeneous nucleation event. As domains grow, they become spherulitic, because the polymers can bend even though the heterogeneously nucleated polymers are roughly parallel initially (7). It is clear that domain structure, which is highly sensitive to conditions of formation, might play a role in rheology.

The above issues could be addressed by microrheological measurements. Red cells themselves would be the logical entities for study, and indeed pipette aspiration or filtration has been used to explore cell rigidification (8–10). A much higher stiffness is found in those studies than in the work on gels, with measured effective shear moduli around 100 kPa. In some cases, the cells become too stiff to be deformed or to pass through filters, so no quantitative

Submitted October 22, 2009, and accepted for publication April 27, 2010.

*Correspondence: fferrone@drexel.edu

Mikhail N. Zakharov's present address is Department of Endocrinology, Diabetes, and Nutrition, Boston University School of Medicine, Boston, MA 02118.

Editor: Edward H. Egelman.

0006-3495/10/08/1149/8 $2.00

doi: 10.1016/j.bpj.2010.04.079

information can be derived. In the oxygenated state, Hb appears to be soluble at all known concentrations, but when cells are deoxygenated, they become incapable of deformation under the pressures used, thwarting attempts to measure the relevant shear or Young's modulus. Thus, we sought to find a method by which we could obtain a significant range of quantitative information about hemoglobin gel deformability on small size samples, and to determine how, if at all, gel rigidity responds to differences in gel structure.

The method we have devised uses laser photolysis of COHbS to create regions of deoxyHbS and sustain them indefinitely. The photolysis technique permits us to create full or partially deoxygenated samples of high-concentration HbS, and to adjust the speed and manner of deoxygenation to favor different domain morphologies (6). Adapting a method we recently employed for analysis of the terminal concentration of polymerization (11), we created small droplets by forming an emulsion of HbS. Compressing the droplets widens their area, which could be measured by image analysis and converted to a change in thickness, since Hb droplets are incompressible. Because area can be measured quite accurately, this method makes it possible to discern nanometer changes in thickness of the sample.

An important variable is the final concentration of polymerized HbS in the droplet. Recently, we found that only around two-thirds of the expected amount of Hb polymer actually forms (12) in purified HbS solution. It was therefore imperative that we measure the final concentration rather than infer it. We did this by masking a small region of the droplet from photolysis. Fig. 1 *a* shows the sample geometry. The area masked, as seen in the bottom of the droplet that occupies the upper left corner, acts as a reservoir for monomers, which cease their flow once polymers can no longer elongate. Separate droplets were used for measuring the change in thickness (reporter droplets) and for photolysis (target droplets). To compress the emulsion, it was placed on top of a rectangular microscope coverslip, and a circular coverslip was placed on top of the emulsion. A small nickel ring was attached to the circular coverslip. (Fig. 1 *b*) Electromagnets placed below the slide could thus create a force on the upper nickel ring and thereby compress the sample as desired.

We find a particularly simple result for multidomain samples. In those cases, the Young's modulus for the gel depends primarily on the concentration of polymerized hemoglobin formed. As we show, this simple result also admits to a simple model for its description. In contrast, gels with a domain morphology that favors larger and fewer domains are softer, as well as more dependent on the concentration of gelled Hb.

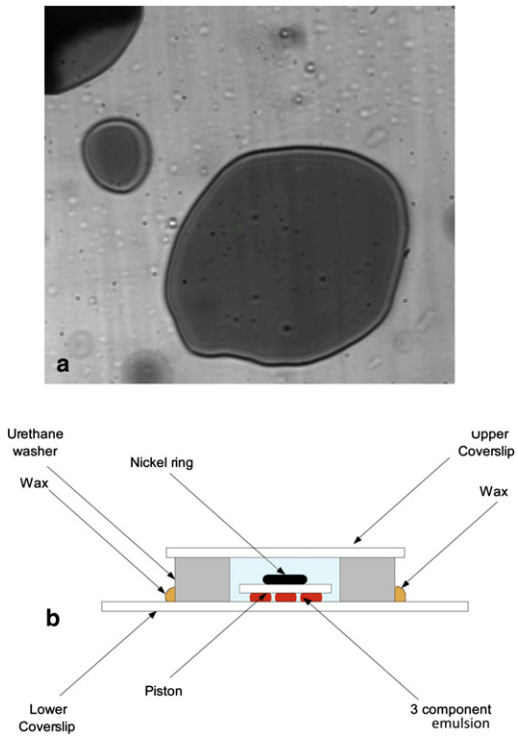

FIGURE 1 (*a*) Typical droplet arrangement, viewed at 432 nm. The large droplet central to the picture is the reporter droplet, whose thickness change will be measured by observing the change in area of its image. In the upper left corner is the target droplet, which has been photolyzed and subsequently has polymerized. The dark region shows the enhanced absorbance from deoxyHb at this wavelength. The lighter gray region is the reservoir, an area that was not photolyzed because the laser was masked and did not illuminate that segment. The reservoir contributes monomers to the gel until the monomer concentration in the gel equals that in reservoir. (*b*) A side schematic of the sample holder (not to scale). A urethane washer is attached to a coverslip, and in its center is placed an emulsion of COHbS in castor oil, suspended in turn in heptane. On top of the emulsion is placed a round coverslip, called the piston, to which a nickel ring has previously been glued. The remainder is filled with heptane, and an upper coverslip is sealed to the top. The thickness of the emulsion is typically ~5 μm. Magnets placed below the sample holder pull on the nickel ring, compressing the sample.

MATERIALS AND METHODS

Purified sickle hemoglobin was prepared according to procedures described previously (6). A small volume of COHbS (typically ~5 μl) was mixed in a vial with 1 μl of castor oil (previously flushed with CO). CO-flushed heptane (~1 ml) was added to the vial, and the resulting mixture was aspirated repeatedly into a micropipette until it formed a three-component emulsion, of which <1 μl was then used in our sample chamber. In previous tests, we observed that nucleation rates, which are highly sensitive to concentration, were unaffected when Hb was encased in castor oil (11).

The sample chamber was constructed from a rectangular coverslip onto which a circular polyurethane washer (~0.1 in thick) was mounted with Kerr sticky wax. A drop of the hemoglobin emulsion described above was placed in the center of the washer. A round coverslip with a diameter less than the inner diameter of the polyurethane washer was placed on the drop. This formed a kind of piston for compressing the sample. When the top coverslip was in place, a few milliliters of heptane were added to the surface of that coverslip, essentially filling the interior space of the washer. Before being placed on the drop, the upper coverslip had had a nickel washer attached to its surface (the side not in contact with the hemoglobin emulsion). Finally, a third coverslip was added to the top of the washer; this coverslip was larger than the inner diameter of the washer and thus formed an external seal (see Fig. 1 *b*).

The apparatus was a Koehler-illumination microscope constructed on an optical table. The stage temperature was thermoelectrically controlled, and feedback was achieved via the control computers. A triangular array of electromagnets was positioned below the sample, and the current through the electromagnets was also computer-controlled. The force applied by the magnets to the nickel ring was mechanically calibrated and found to be linear in the current applied.

The illumination beam was from a 150-W xenon arc lamp passed through an Acton f/4 monochromator (Acton Research, Acton, MA). The microscope used a Leitz 32× long working distance objective and a second identical objective as the condenser.

Detection was via a two-camera system positioned after a beam splitter. For spectra, we used a Photometrics (Tucson, AZ) CH350 system that had ~70% quantum efficiency and 14-bit conversion; for rapid image analysis, including widening measurements, we used a Fastcam (PCI-512, Photron, San Diego, CA) that has ~10-fold less quantum efficiency and 8-bit conversion.

Photolysis was achieved by illuminating the sample using a 5-W 2020 argon ion laser (Spectra-Physics, Mountain View, CA) operated at 488 nm. Power was monitored by picking off a part of the beam with an optical wedge. Light from the laser was injected into the optical path by a low-pass dichroic mirror placed in the optical path before the condenser, and was kept from reaching the cameras by a notch filter. Intensity was kept only high enough to insure complete photolysis, unless otherwise indicated (see Results).

Spectra were collected by stepping the monochromator and obtaining an image of the sample at 1-nm intervals between 400 and 450 nm. To keep the image in focus, the objective was repositioned at each wavelength by computer control of a small piezo-driver picomotor (New Focus, San Jose, CA) attached to a micrometer stage on which the objective was mounted. In a separate calibration run, the optimum displacement was determined using an entropy-based focus algorithm. An absorption spectrum could thus be assigned to each pixel in the resulting image. The spectrum was fit using standard known spectra of deoxyHb, COHb, and metHb. This allowed a spatial map to be constructed of various sample components in the image plane. Samples used for study never had >5% metHb, approximately the threshold of its detection in our droplets.

Sample compression was measured by observing the area of a reporter droplet in monochromatic light of wavelength 425 nm. The transmitted intensity was converted to absorbance before the image was processed to determine thickness changes. A fast filling algorithm was employed to determine the droplet area. Typical sample thickness was ~5 μm.

RESULTS

Compression of COHbS emulsions showed linear dependence of deflection on the driving force, i.e., Hookean behavior (Fig. 2). In this and all other experiments, to insure that no irreversible changes were occurring, data points were collected by choosing the driving forces in random sequence rather than in a monotonic sequence. There was a 2-min interval between all force measurements in the sequence. The points were fit to a straight line constrained to pass through the origin, and the force constant was the inverse of the slope. To convert the force constant to the Young's modulus, it was multiplied by the sample path length (determined by measuring spectra) and divided by the area of the droplet.

Upon laser photolysis, samples were notably less deformable as the stiffness increased well above the detection limit. Typical results are shown as red points in Fig. 2, all lying below the points taken without photolysis. Samples with a gelled droplet also were compressed in random sequence of forces, and responded in a Hookean fashion. Again, the data was fit to a line constrained to pass through the origin, to obtain the inverse force constant. We assumed the unphotolyzed system and gelled area functioned as parallel springs, so that the difference in force constants gave the force constant that was appropriate to the gelled droplet alone.

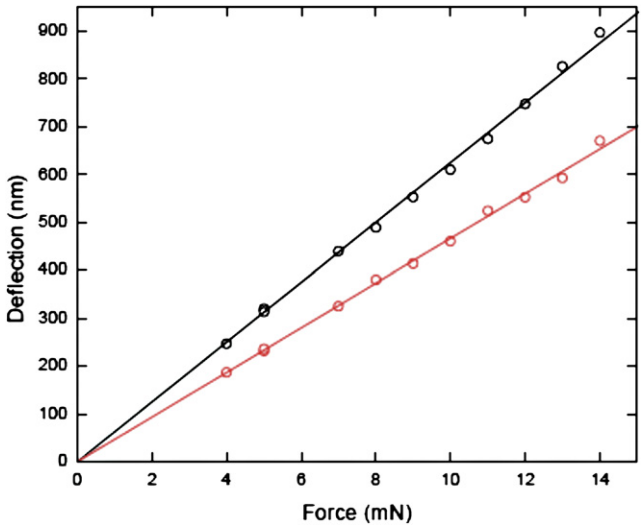

FIGURE 2 A typical response of droplets to compression. In each case, forces were chosen at random, and the deflection was measured by observing the area of the reporter droplet. Note the high accuracy and repeatability provided by this method. The upper (*black*) points were measured without photolysis and thus represent the elastic response of the whole slide. The lower (*red*) points were measured with laser photolysis and show the diminished compressibility of the sample when a single droplet has been photolyzed. Points were fit by a straight line constrained to pass through the origin. The upper (control) slope was 52.5 ± 0.4 nm/mN, whereas the lower slope was 46.6 ± 0.3 nm/mN. The sample concentration was 29.1 g/dl, and measurements were performed at 25°C.

To monitor final concentrations of HbS when the sample was photolyzed, an area amounting to no more than a few percent of the droplet was masked from the photolysis beam by obstructing the laser beam in a place in the beam path conjugate to the sample plane. Absorbance spectra were measured pixel by pixel in the image. Upon photolysis, the absorbance in this area decreased as monomers diffused into the polymerized region. When absorbance in the masked area reached a stable value, polymerization was taken to be complete. Full photolysis was considered to be achieved when the relative content of deoxyHbS in the photolyzed area exceeded 95%. Typical uncertainty is 5%, and this is largely due to the small observation areas, since spectra are taken pixel by pixel. Birefringence was also normally apparent when the sample was viewed between crossed polarizers. The amount of polymerized HbS was thus taken as the difference between the initial concentration of COHbS and the terminal concentration of HbS evaluated when polymerization was taken to be complete.

TABLE 1 Young's modulus (Y) measured under various conditions

c_o (g/dl)	T (°C)	Setup*	Photolysis%	Δ (g/dl)†	Y (kPa)
29.1	25	Stepped	100	8.7	315
29.1	25	Stepped	100	8.8	500
32.4	25	Stepped	100	8.5	564
32.4	25	Stepped	100	9.0	579
32.4	25	Stepped	100	8.8	671
34.4	25	Stepped	100	9.3	685
34.4	25	Stepped	100	9.5	809
34.4	25	Stepped	100	9.9	983
29.8	20	Full	100	8.8	907
28.9	25	Full	75	6.1	282
28.9	25	Full	94	8.8	443
30.2	25	Full	75	7.2	331
30.2	25	Full	94	9.3	612
34.1	25	Full	75	6.8	492
34.1	25	Full	94	8.6	750
28.9	25	Full	100	9.7	1171
29.1	25	Full	100	9.6	869
29.8	25	Full	100	9.9	1141
29.1	25	Full	100	9.0	654
30.2	25	Full	100	11.8	1192
32.4	25	Full	100	10.2	1034
32.4	25	Full	100	10.5	1133
32.4	25	Full	100	11.0	1142
33.6	25	Full	100	11.1	1304
34.1	25	Full	100	11.3	1382
34.1	25	Full	100	11.2	1475
34.4	25	Full	100	11.5	1479
34.4	25	Full	100	10.9	1364
34.4	25	Full	100	9.5	718
29.8	30	Full	100	10.1	1201
33.6	30	Full	100	11.7	1451
34.1	30	Full	100	11.7	1500

*Stepped indicates that a small region was first photolyzed and then expanded to include the entire drop (less the masked areas). Full indicates that the entire drop was immediately subject to the laser illumination.
†Δ is the final concentration of polymerized Hb.

Experiments were carried out for initial HbS concentrations between 28.9 and 34.4 g/dl (tetramer) at temperatures from 20 to 30°C. The results are listed in Table 1 and shown in Fig. 3. The data at 20°C are shown as triangles, those at 25°C as circles, and those at 30°C as diamonds. Higher initial HbS concentrations are shown by darker symbols. The solid curve is from the theory described below. The values of Y are clearly dominated by a single variable, viz. the value of the final concentration of polymerized deoxyHbS, rather than either the initial concentration or the temperature of the experiment.

A series of experiments were executed in which the initial photolysis level was below that required for full photolysis. Note that the final concentrations of HbS have been measured, and all are lower than the values expected from the photolysis level. The results of these experiments are shown in Fig. 4. As in Fig. 3, darker symbols correspond to higher initial concentrations. It is apparent that most, though not all, of the partial photolysis experiments have a Young's modulus lower than that found in the full photolysis experiments.

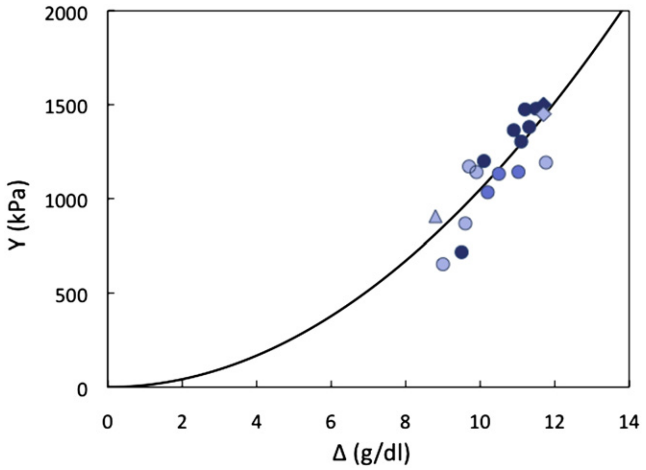

FIGURE 3 Young's modulus as a function of the concentration of Hb that is polymerized for samples that were fully photolyzed. Data taken at 20°C are represented by triangles, those at 25°C by circles, and those at 30°C by diamonds (see Table 1). Higher concentrations are indicated by darker symbols. The solid curve is the best fit to the simple theory (Eq. 1) derived in the Appendix.

Finally, a series of experiments was carried out in which an iris diaphragm was used to limit the photolysis area to a circle with a diameter of 5 μm, much smaller than that of the target droplet (~80 μm). Once this region was photolyzed, after the concentration in the masked area stabilized, the diaphragm was opened to bring the photolysis beam to a size larger than the droplet while still retaining a small masked area. Thus, although the final state of the sample (fully photolyzed) was the same, the path to achieving it

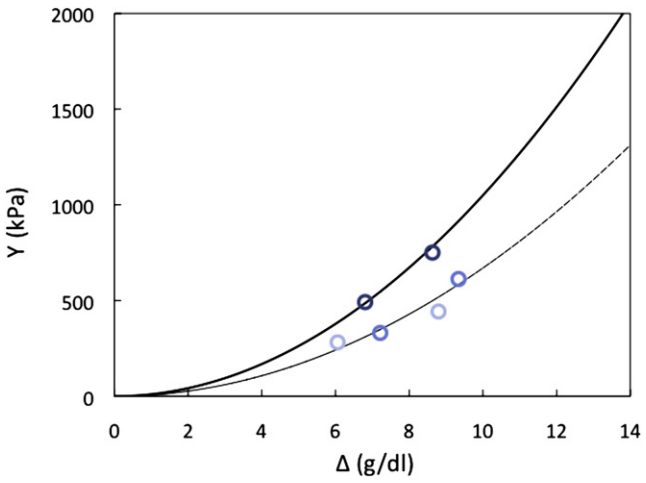

FIGURE 4 Young's modulus as a function of the concentration of Hb that is polymerized for partially photolyzed samples. All data were collected at 25°C (see Table 1). Higher concentrations are indicated by darker symbols. The solid curve is the best-fit theory for the full-photolysis experiments of Fig. 3, and it accurately fits some but not all of the data. The lower concentrations were also fit by Eq. 1 with a smaller value of a, which we interpret as the consequence of a different internal gel structure.

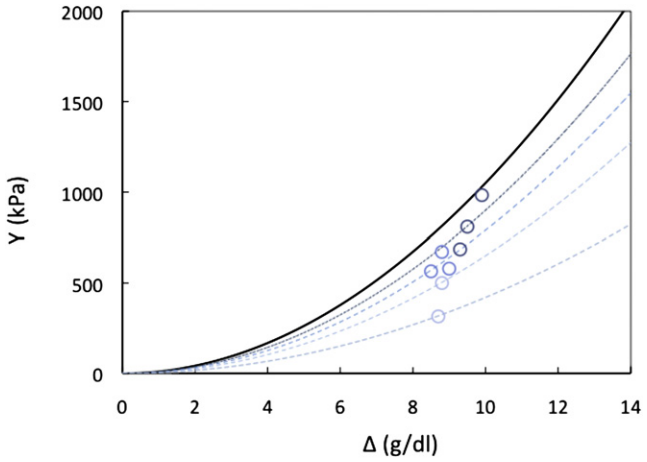

FIGURE 5 Young's modulus as a function of the concentration of Hb that is polymerized for experiments in which an iris masked the initial photolysis area but was subsequently opened to illuminate the entire droplet. Thus, full photolysis was created but with a different underlying gel structure than that seen in the experiments represented in Fig. 3. All data were collected at 25°C (Table 1). The higher the concentration is, the darker the symbols are. The solid curve is the fit to the full-photolysis data of Fig. 3 and lies above the data shown. Dashed curves using different a values are drawn to illustrate the difference that gel formation can generate.

was different. Opening the iris was expected to create a gel with regions of aligned fibers where the central region first expanded, since fibers grow faster than they nucleate. In regions near the periphery, however, nucleation may still occur, because the characteristic nucleation times are shorter than the time needed for growing fibers to reach the edges. In all cases, the final concentration was lower when photolysis in a small spot was followed by aperture opening than when the whole area was photolyzed at once. For example, at 25°C and 34.4 g/dl, when the full area was photolyzed immediately, 9.5 g/dl of polymer formed, whereas only 8.6 g/dl of polymer formed when polymerization began in a small area and was allowed to subsequently fill the whole area. The Young's modulus measured in these experiments is shown in Fig. 5, again with higher initial concentrations indicated by darker symbols. Even more so than in partial photolysis experiments, the values of the Young's modulus are lower than those observed for fully photolyzed samples containing the same amount of polymer.

DISCUSSION

To interpret the results, it is helpful to understand the underlying polymer domain structure, particularly the substantial interpenetration of domains. Each domain is a structure that begins with a homogeneous nucleation event from which a fiber grows and is followed by multiple heterogeneous nucleation events that generate further fibers. As fibers bend, the domain expands about the axis of the original fiber; as monomers are consumed in the polymer mass, new monomers diffuse into the region of the growing gel. The number density of domains reflects the extraordinary concentration dependence of homogeneous nucleation, viz. 50th order or higher (13), and therefore can vary dramatically as conditions are changed. In the full-photolysis experiments described here, the number of homogeneous nuclei expected to form in the sample volume ranges from 10^4 to 10^7. Christoph et al. (14) found that the number of homogeneous nuclei exceed the actual number of domains observed, in general by more than a factor of 10, since domains occupy space that otherwise would have been available for further nucleation. Consequently, the full-photolysis experiments reported here are estimated to contain 10^3 to 10^6 domains. Although the spacing of domains depends on the underlying homogeneous nucleation, their extent depends on polymer growth. Under these conditions, the average polymer length grows to the periphery of the average domain after ~10% of the reaction. Thus, the remaining 90% of polymer lengthening occurs in the space of other domains. Even with the occlusion of polymer ends by other polymers, domains will extensively interpenetrate one another under the conditions of full photolysis seen here. Consequently, a gel in multidomain samples will be dominated by interwoven polymers, despite their origin as a separated array of domains.

When the laser intensity is reduced to yield only partial photolysis, nucleation will be reduced more than growth since nucleation is more concentration-dependent than growth. This will thus give a greater spacing to domains relative to the final polymer length.

Final concentrations of polymerized hemoglobin measured in partial-photolysis experiments are consistent with these domains having an altered internal structure. Consider the experiment in which the laser was reduced to 75% of full power. Had desaturation been linear in laser power, 0.75 of the full-power deoxyHbS would be formed. In fact, ~0.85 deoxyHbS is seen at that power level (6,15). The deoxyHbS will then polymerize. Since solubility increases only slightly under these conditions of partial saturation, at least 0.80 of the full-photolysis polymer mass ought to have formed, yet only 0.60 of the full-photolysis polymer mass was actually formed. We interpret this deficit of polymer mass at lowered laser intensity as the consequence of a different local geometry, which plays a role in determining the net polymer mass, due to end obstruction (11,12). In short, not only do fewer polymers form, but they form in a somewhat different geometry.

The iris experiments also create a different local geometry. The photolysis of the central 5-μm-diameter spot allowed a multidomain region to be formed that occupied only 0.4% of the sample area. Based on previous measurements, we expected that if we waited till that region saturated, Hb diffusion into the central region would generate a densely packed gel of 45–55 g/dl concentration (16,17), and that when the iris was then opened rapidly, polymer growth around the center would generate a region of relatively

aligned radial polymers. Because polymer growth rates are of the order of 5 μm/s, these existing polymers would reach the droplet periphery in ~7 s. However, the tenth time of the sample is 1–2 s, implying that the periphery of the droplet will polymerize spontaneously before the arrival of the fibers generated in the high-density core. Again, we expect to see a region of polymers with greater than average alignment. When this is compared directly with samples that were fully photolyzed all at once, it displays less polymerization, as discussed in the Results section.

A simple lattice model for the Young's modulus can be developed to relate the modulus to the polymerized hemoglobin concentration. As derived in the Appendix, the Young's modulus of the gel network is proportional to the square of the concentration of polymerized Hb concentration, Δ.

$$Y = a\Delta^2 \tag{1}$$

The constant a depends on the character of the constituent gel, viz. the Young's modulus of the individual fibers, as well as their geometry. Because of the difficulty of specifying the geometry and the complexity of a more realistic calculation, the exact constants that enter into a are not specified. Equation 1 is fit to the full-photolysis data in Fig. 3, and that fit curve is duplicated as the solid line in Figs. 4 and 5. As can be seen, it provides a good representation of the data in Fig. 3. Furthermore, a less cross-linked (i.e., less interwoven) structure would be expected to have a smaller value of a, and this is seen in Figs. 4 and 5. It is interesting to note, in Fig. 4—which describes the partial-photolysis experiments, that the higher-concentration data (34.1 g/dl) are well fit by the same curve that describes full photolysis, suggesting that the changes in nucleation did not substantially change the underlying gel for that concentration. The lower concentrations (30.2 g/dl and 28.9 g/dl) are well described by a curve with a lowered value of a, but one not significantly different for the two concentrations. This most likely reflects that the Young's modulus is only expected to change by ~6% between the two data points, and that variations in structure might occur at this level. In Fig. 5, certain duplicate experiments differ by ~40%, which we again attribute to variation in the structure of the gel, which is more likely in the iris experiments. Note that this variation is not a general feature of the method itself, since in full photolysis, variation in a triplicate set of experiments was only ~5%. It does serve to emphasize that when the domain structure is densely uniform, the values of the Young's modulus are well predicted, whereas when the domain structure is less uniform, the Young's modulus varies and diminishes. It remains to be determined what Young's modulus would be for a single-polymer domain.

The magnitude of the Young's modulus is notably higher than has been observed previously. To obtain the Young's modulus from shear modulus data requires multiplying the latter by a factor of 3, assuming an incompressible gel. Previous data suggest that Y ~1 kPa, which, on the scale shown in Fig. 3, would be indiscernibly above the abscissa. It is clear that single-cell data would be higher, but it is hard to know where to place such data on the concentration axis for comparison, since the methods used on cells can only explore cells that are partially deoxygenated, since only these cells retain enough flexibility to be observed in aspiration or filtration experiments. Therefore, it is possible that cellular experiments are consistent with the results shown here. However, the existing bulk shear data are clearly not consistent with either the data described here or the cellular data.

These results provide important quantitative insights into the process of vasoocclusion. Consider the case where the final oxygen saturation is 50%, and the typical arteriovenous pressure difference is 3.2 kPa (24 mm Hg). At equilibrium, a multidomain cell would contain ~5.3 g/dl of polymer and exhibit a modulus of ~300 kPa, implying that the in vivo pressure difference would lead to a mere ~1% strain. Were equilibrium reached within the capillary, a cell that could compress by no more than 1% amounts to occlusion. This is because the outward force of the mass of polymers would ensure that an erythrocyte expanded to the widest part of the capillary, even slightly deforming the capillary walls (11), and the cell's rigidity would ensure that it could not be subsequently recompressed. On the other hand, had the cell only reached its 10% value (i.e., its tenth time, or delay time), it would have a modulus 100 times smaller, and deformation would be a simple matter. Therefore, obstruction would occur only if the delay time were exceeded while the cell was in the capillary. This represents the validation of a central tenet of the classic kinetic hypothesis that holds that intracapillary sickling would equal occlusion (18), although a precise limit cannot yet be established as to the necessary fractional extent of the reaction. More recent in vivo studies on the pathophysiology of sickle cell disease found evidence for adhesion of erythrocytes and/or leukocytes, behind which multiple sickled cells would create an occlusion (19,20). It is clear from the above values that once the delay time is past, the cells rapidly become rigid objects. This could allow a group of cells arriving at a partial obstruction, such as an adherent erythrocyte or leukocyte, to become jammed (21), providing a quantitative rationale for the observations. Most interesting is an intermediate case. If one supposes that a 10% deformation would permit cells to slip past one another, those cells would require a modulus in the range of 30 kPa, a value achieved with only ~1.7 g/dl of polymer. Thus, for example, to melt an obstruction would require substantial oxygenation, viz. ~75% saturation if one takes the 10% deformation as a normative value for escape.

Finally, it must be recognized that the viscoelasticity of a gel has two components, and that only the elasticity has been determined here. Qualitatively, it is evident that a large viscous component would make cells even less deformable at the point of encounter with an obstruction, until at some

time following the encounter the cell's deformation finally occurred. The relaxation to permit cells to escape the early phases of an occlusion would thus be highly sensitive to the gel viscosity and rate at which the gel (and its underlying structure) evolved. It is clear that the viscous and elastic criteria for motion of cells past one another represent another important line of investigation that will need to be pursued to complete the connection between rheology and vasoocclusion.

APPENDIX

We consider an isotropic, homogeneous, cross-linked gel comprised of unstrained, cross-linked fibers. Our interest is in using this as a model for the elastic properties of a dense gel of sickle hemoglobin fibers. The gelation transition in sickle hemoglobin solutions is highly first-order and therefore tends to produce inhomogeneous gels that are quenched in the sense that subsequent reordering transitions from fiberlike to crystalline packings occur only on much longer experimental timescales. Since in the large system size limit these gels are expected to be globally isotropic, we seek a model of an isotropic cross-linked fiber network. We will further idealize by assuming that the gel is also homogeneous. The simplest candidate for this is a model in which the fibers are arranged in a cubic lattice. We expect this model to be qualitatively accurate independent of the microscopic geometry of the gel and to yield semiquantitative estimates for, e.g., the modulus of the gel. The geometry of the gel may lead to differences in the density of polymers, but the scaling of the modulus, which we will see is proportional to concentration squared, should not be affected. The differences are in the prefactor, or constant of proportionality, which can be determined experimentally and which one might not expect to vary by more than a factor of 10 due to geometric effects. It is in that sense that our estimates are semiquantitative.

Thus, our motivation is to determine how the Young's modulus for the gel will depend on the concentration of monomers contained in the gel. Such a relationship is independent of the detailed model of the gel in that it is fundamentally a search for the way in which the modulus scales with the gel concentration. To emphasize such features, therefore, the derivation that follows will systematically remove prefactors that are detail-specific to retain general features that will scale regardless of the details. It is the same approach by which the volume of an unspecified object might be said to resemble the product of its length, width, and height, even if the specific shape is not the box for which this product is rigorously the volume.

For simplicity of analysis, we begin by considering a small shear strain, ε, applied to the model cubic mesh of sickle fibers, which in turn gives rise to corresponding strains in the constituent fibers between cross-links (see Fig. 6). Thus, these sections of fiber become S-shaped. The mean curvature in each fiber is of the order of the strain divided by the segment length. Thus, for a mesh with lattice spacing ξ, if R is the radius of curvature, each fiber has an average curvature, $1/R$, of the order of ε/ξ . This gives u, the energy of each fiber, which is the integral of the squared curvature multiplied by (half) the rigidity, κ, that is therefore

$$u \sim \kappa\xi(\varepsilon/\xi)^2,$$

since the curvature has been taken as an average value over the length ξ .

The energy/unit cell is the number of fibers in a cell multiplied by the fraction of each fiber in that cell. Thus, $U = 3u$. In the scaling approximation, then, $U \sim u$. The Young's modulus, Y, is equal to the energy density, U/V, divided by the squared strain, ε^2. Thus,

$$Y \sim \kappa/\xi^4.$$

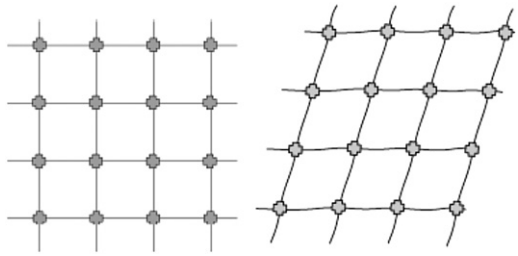

FIGURE 6 A sketch of a simple cubic fiber gel of mesh size ξ. Cross-links, roughly equivalent to entanglement, are shown as cross-shaped symbols. (*Left*) Unsheared state. (*Right*) After shear. Note that the sections of fiber between cross-links are strained into an S-shape by the shear.

We can relate the mesh size, ξ, to Δ, the concentration of polymerized Hb, as follows. There is a total length of fiber in one mesh volume of 3ξ following the same arguments by which energy was divided among cells. If λ is the amount a fiber lengthens per monomer, then the number of monomers contained in each mesh volume is $\sim\xi/\lambda$. Thus, the concentration, Δ, which is simply the number of monomers/volume V, is $\sim 1/(\lambda\xi^2)$, and we obtain the modulus

$$Y \sim \lambda^2\kappa\Delta^2.$$

The rigidity, which is in fact the quantity directly measured, is given by $\kappa = Y_o I$, where Y_o is the Young's modulus of individual fibers (5), which is in the range 50–100 MPa. I is the moment of the fiber, which is $^1/_8\pi b^4$ for a cylindrical fiber of radius b. If A is the cross-sectional area of the fiber, $I = A^2/8\pi$. It follows that

$$Y \sim Y_o(\lambda A)^2\Delta^2,$$

where λA is the volume of a single-molecule-thick slice of the fiber. λA consists of 14 molecules of specific volume $1/c_{fib} = 1/69$ (g/dl)$^{-1}$ in the polymer. (Polymer density is lower than individual monomers because of the spacing within a fiber.) Thus,

$$Y \sim Y_o\Delta^2/\left(c_{fib}\right)^2.$$

This argument has identified the physical features by which the modulus of the gel scales, and it makes clear that the individual fiber Y_o sets the elementary scale, and that the concentration of monomers contained in the fiber must be squared in accounting for variance in Y. The excised prefactors would manifest the particular details, such as the specific geometry of the gel. The detailed analysis of such an effect would require substantial descriptive information regarding the gel that does not presently exist, and moreover would entail a substantially more complex calculation to account for the various gel microscopic anisotropies. One further geometric aspect should be mentioned, viz. that the constituent fibers might appear in bundles. In that case, for example, the fiber radius, b, would also be different, although this would not affect the scaling relationships.

Therefore, the essential scaling relationship can be expressed as

$$Y = \alpha Y_o\Delta^2/\left(c_{fib}\right)^2 = a\Delta^2,$$

where α is a constant that reflects the underlying geometry. Because of the dependence of α on geometry, even though it is unknown, its variation can traced to changes in the geometry, as is done in the text. Finally, note that the derived relationship treats the Young's modulus and shear modulus as interchangeable, since they would only differ by a factor that can be folded into the constants above.

The authors thank Prof. Robin Briehl for helpful discussions and Suzanna Kwong for assistance in sample preparation.

This work was supported by National Institutes of Health grants R01 HL057549 and P01HL058512.

REFERENCES

1. Briehl, R. W. 1980. Solid-like behaviour of unsheared sickle haemoglobin gels and the effects of shear. *Nature.* 288:622–624.
2. Gabriel, D. A., L. A. Smith, and C. S. Johnson, Jr. 1981. Elastic properties of deoxy hemoglobin S (deoxy-HbS) gels. *Arch. Biochem. Biophys.* 211:774–776.
3. Danish, E. H., J. W. Harris, …, I. M. Krieger. 1987. Rheologic behavior of deoxyhemoglobin S gels. *J. Mol. Biol.* 196:421–431.
4. Wang, J. C., M. S. Turner, …, R. W. Briehl. 2002. Micromechanics of isolated sickle cell hemoglobin fibers: bending moduli and persistence lengths. *J. Mol. Biol.* 315:601–612.
5. Turner, M. S., …, R. W. Briehl, R. Josephs. 2006. Anisotropy in sickle hemoglobin fibers from variations in bending and twist. *J. Mol. Biol.* 357:1422–1427.
6. Ferrone, F. A., J. Hofrichter, and W. A. Eaton. 1985. Kinetics of sickle hemoglobin polymerization. I. Studies using temperature-jump and laser photolysis techniques. *J. Mol. Biol.* 183:591–610.
7. Dou, Q., and F. A. Ferrone. 1993. Simulated formation of polymer domains in sickle hemoglobin. *Biophys. J.* 65:2068–2077.
8. Kraiem, A., C. T. Craescu, …, Y. Beuzard. 1989. Filterability of sickle cells as a function of pO2: role of physico-chemical factors. *Biorheology.* 26:771–784.
9. Mackie, L. H., and R. M. Hochmuth. 1990. The influence of oxygen tension, temperature, and hemoglobin concentration on the rheologic properties of sickle erythrocytes. *Blood.* 76:1256–1261.
10. Itoh, T., S. Chien, and S. Usami. 1995. Effects of hemoglobin concentration on deformability of individual sickle cells after deoxygenation. *Blood.* 85:2245–2253.
11. Aprelev, A., W. Weng, …, F. A. Ferrone. 2007. Metastable polymerization of sickle hemoglobin in droplets. *J. Mol. Biol.* 369:1170–1174.
12. Weng, W., A. Aprelev, …, F. A. Ferrone. 2008. Universal metastability of sickle hemoglobin polymerization. *J. Mol. Biol.* 377:1228–1235.
13. Cao, Z., and F. A. Ferrone. 1996. A 50th order reaction predicted and observed for sickle hemoglobin nucleation. *J. Mol. Biol.* 256:219–222.
14. Christoph, G. W., J. Hofrichter, and W. A. Eaton. 2005. Understanding the shape of sickled red cells. *Biophys. J.* 88:1371–1376.
15. Galkin, O., R. L. Nagel, and P. G. Vekilov. 2007. The kinetics of nucleation and growth of sickle cell hemoglobin fibers. *J. Mol. Biol.* 365:425–439.
16. Cho, M. R., and F. A. Ferrone. 1990. Monomer diffusion into polymer domains in sickle hemoglobin. *Biophys. J.* 58:1067–1073.
17. Cho, M. R., and F. A. Ferrone. 1992. Monomer diffusion and polymer alignment in domains of sickle hemoglobin. *Biophys. J.* 63:205–214.
18. Eaton, W. A., J. Hofrichter, and P. D. Ross. 1976. Editorial: Delay time of gelation: a possible determinant of clinical severity in sickle cell disease. *Blood.* 47:621–627.
19. Kaul, D. K., M. E. Fabry, and R. L. Nagel. 1989. Erythrocytic and vascular factors influencing the microcirculatory behavior of blood in sickle cell anemia. *Ann. N. Y. Acad. Sci.* 565:316–326.
20. Turhan, A., L. A. Weiss, …, P. S. Frenette. 2002. Primary role for adherent leukocytes in sickle cell vascular occlusion: a new paradigm. *Proc. Natl. Acad. Sci. USA.* 99:3047–3051.
21. Liu, A. J., and S. R. Nagel. 2001. Jamming and Rheology. Taylor and Francis, New York.